Low frequency variability in an coupled ocean-sea ice general circulation model of the Southern Ocean

Terence J. O'Kane[1] Richard J. Matear[2]
Matthew A. Chamberlain[3] James S. Risbey[4]
Ilia Horenko[5] Bernadette M. Sloyan[6]

(Received 9 October 2012; revised 12 April 2013)

Abstract

A coupled ocean-sea ice general circulation model is used to identify a Southern Ocean southeast Pacific intrinsic mode of low frequency variability and its response to interannual atmospheric forcing. Using forcing data from the co-ordinated ocean-ice reference experiment, a comprehensive suite of experiments elucidated excitation and amplification mechanisms of this intrinsic mode by low frequency forcing and stochastic forcing due to high frequency winds. Subsurface thermocline anomalies are found to teleconnect the Pacific and Atlantic regions of

http://journal.austms.org.au/ojs/index.php/ANZIAMJ/article/view/6178 gives this article, © Austral. Mathematical Soc. 2013. Published May 26, 2013, as part of the Proceedings of the 16th Biennial Computational Techniques and Applications Conference. ISSN 1446-8735. (Print two pages per sheet of paper.) Copies of this article must not be made otherwise available on the internet; instead link directly to this URL for this article.

the Antarctic circumpolar current (ACC). It is found that the Pacific region of the ACC is characterised by intrinsic baroclinic disturbances that respond to both zonal and latitudinal wind variations, while the Atlantic sector of the ACC is sensitive to higher frequency synoptic winds that act to amplify thermocline anomalies propagating downstream from the Pacific resonant with eastward travelling Rossby waves. This simulation study identifies plausible mechanisms that determine the predictability of the Southern Ocean climate on multi-decadal timescales.
Subject class: 76
Keywords: intrinsic, forced and low frequency ocean modes

Contents

1 Introduction

The Southern Ocean encircles the globe and has large variability with a considerable low frequency component. The Southern Ocean directly links all

the major ocean basins, allowing water mass exchange at depths shallower than the Drake Passage via the eastward flowing Antarctic circumpolar current (ACC). Interannual variability is often observed at high southern latitudes. Observations of oceanic Rossby waves [3] suggest that such features propagate eastwards around the Southern Ocean. Hughes [3] modelled Rossby waves in the Southern Ocean and showed that they occur at a natural scale of approximately 300 km, and in two distinct regions: within the ACC (strong interaction with the mean flow and eastward propagating with the current); and outside the ACC (nearly linear and westward propagating). Their study divided the Southern Ocean into two dynamical flow regimes: subcritical and supercritical with regard to the wave speed. The eastward travelling waves point along the direction of the mean flow, acting to accelerate the eastward flowing jets.

Dijkstra and Ghil [2] showed that intrinsic oceanic mechanisms, under certain conditions, exhibit strong low frequency variability in highly nonlinear western boundary current extensions. Quattrocchi et al. [9] introduced the concept of coherent resonance to describe the effect of a time dependent wind forcing on the intrinsic low frequency variability of the Kuroshio Extension. While there is a now a body of literature using idealised models to suggest that intrinsic low frequency variability and multiple equilibria due to nonlinear mechanisms internal to the ocean system are present in both the North Atlantic and North Pacific western boundary current extensions, there are few studies that we are aware of using state of the art primitive equation models to study intrinsic processes in the Southern Ocean and the ACC. Therefore, it is of great theoretical and practical interest to investigate how nonlinear internal ocean dynamics contribute to the low frequency variability of the Southern Ocean.

To identify any intrinsic processes or modes capable of producing low frequency variability in the Southern Ocean we use climatological or nominal year atmospheric forcing provided by time independent surface wind stresses. We then take a systematic approach, separately adding to the nominal year forcing the low frequency components of interannual variability due to the

southern annular mode (SAM), the El Niño southern oscillation (ENSO), and higher frequency synoptic weather components. In this manner we identify the mechanisms that drive ocean low frequency variability in the ACC.

2 Experimental configuration

The model is the Australian Community Climate and Earth System Simulator-ocean (ACCESS-O) configuration of the Geophysical Fluid Dynamics Laboratory modular ocean model (version 4p1) and ocean-ice code [1]. Details of our configuration are in Appendix A. This study employs atmospheric fields from the Coordinated Ocean-ice Reference Experiments (CORES) [5] for global ocean-ice modelling. For our experimental configuration we used the CORE.v1 nominal year forcing and the CORE.v2 interannually varying forcing (1948–2007) (hereafter CORE1 and CORE2, respectively).

Intrinsic modes of variability are analysed with CORE1 forcing and interannual variability with CORE2 forcing. In addition to these experiments, we examine the dynamical mechanisms driving the Southern Ocean variability with experiments forced with CORE1 fields plus various combinations of the constituent modes of low frequency variability from the CORE2 data, namely the SAM and the ENSO.

In an empirical orthogonal function (EOF) analysis of tropical sea surface temperature anomalies Timmermann [10] showed that the mature ENSO phase is associated with the first EOF whereas the second EOF mode characterises the zonal displacement of said anomalies. As we move to higher latitudes the SAM dominates the leading mode of atmospheric variability and the latitudinal variations due to ENSO are expressed in the second and third EOFs [8]. Winds over the Southern Ocean from the CORE2 data set were reduced to EOFs. The zonal winds in the experiment testing the SAM mechanism were constructed by adding a twelve month smoothed first EOF component of CORE2 winds to CORE1 over the Southern Ocean south of 30°S, with CORE1 forcing applied

everywhere else. ENSO winds were constructed by adding the second and third EOF components of the CORE2 forcing to the CORE1 fields. The meridional components of the winds were constructed by regressing the zonal winds of the two modes on the full meridional winds. Additional high frequency configurations were used to examine the response to the synoptic weather atmospheric forcing over the Southern Ocean. Two high frequency fields were considered: firstly, CORE2 with the SAM and ENSO variability removed (CORE2−SAM−ENSO); and secondly, a twelve month boxcar filter was applied to the CORE2 winds to remove all low frequency interannual variability. In all 'mode' experiments only the winds are changed and the fluxes appropriately modified using bulk formulas. For the CORE2 a full set of interannually varying forcing fields was used.

3 Diagnostics

Our diagnostics include principal component analysis (PC) to ascertain the temporal variability for each model simulation and forcing configuration. In all cases the seasonal cycle is removed from the anomalies prior to calculating the EOFs and PCs. In order to diagnose whether the growth, relative strength and pathways of ACC anomalies are due to barotropic and/or baroclinic disturbances of the mean flow we examined two mean-transient energy transfer terms: mean kinetic energy (MKE) to transient kinetic energy (EKE) (not shown); mean potential energy (MPE) to transient potential energy (EPE). We express all variables in terms of time means (overbar) and fluctuations (prime). The potential energy transfer term is

$$\text{MPE} \rightarrow \text{EPE} = \left(\overline{u'\rho'}\frac{\partial\overline{\rho}}{\partial x} + \overline{v'\rho'}\frac{\partial\overline{\rho}}{\partial y}\right)\left(\frac{\partial\tilde{\rho}}{\partial z}\right)^{-1} \quad (1)$$

where ρ is the potential density and $\tilde{\rho}$ is the reference state approximated as the horizontal average of the time mean. Scalar fields u and v are the horizontal velocity components with respect to x and y, the zonal and meridional

directions, respectively. These energy transfer terms are calculated using 100 (CORE1) and 60 years (CORE2 and component simulations) of output from the ACCESS ocean-ice configuration. The transfer rate between mean kinetic energy and transient kinetic energy, that is the work of the Reynolds stresses on the mean shear, is associated with growing barotropic disturbances (positive values). Equation (1) is the transfer of mean potential energy to (from) the mean flow. Positive (negative) values of MPE → EPE indicate the generation (dissipation) of potential energy in the mean flow. In general, baroclinic disturbances are found to be up to two orders of magnitude larger than barotropic processes and so we concentrate our discussion on the former.

4 Mechanisms

Potential energy transfers illustrate the role of interannual atmospheric forcing in amplifying intrinsic baroclinic disturbances in the ACC, and in particular in the Pacific. For intrinsic disturbances (CORE1, Figure 1) the region in the Pacific at 150°W of the East Pacific Rise, after the ACC passes through the Eltanin and Udinstev fracture zones, defines the location where the flow is predisposed to being unstable. At this location, low frequency variability in the flow occurs because of the unique topography: steep at the rise and a downstream flat abyssal plain. Figure 1 shows the Drake Passage as a choke point for the eastward propagating baroclinic disturbances that are generated or amplified at the East Pacific Rise and are resonant with the eastward propagating Rossby waves. These intrinsic baroclinic disturbances are typically of an order of magnitude weaker than those found in the CORE2 simulation, but are typically of larger scale and more coherent (that is, less variable) in the ACC.

The timescale of the CORE1 intrinsic mode is seen in the leading principal components (PCs) of temperature at 200 m (T200) (Figure 2, row two). The mode is characterised by an oscillation between warm and cold states with a 20 year period. The growth and decay cycle of baroclinic instability about

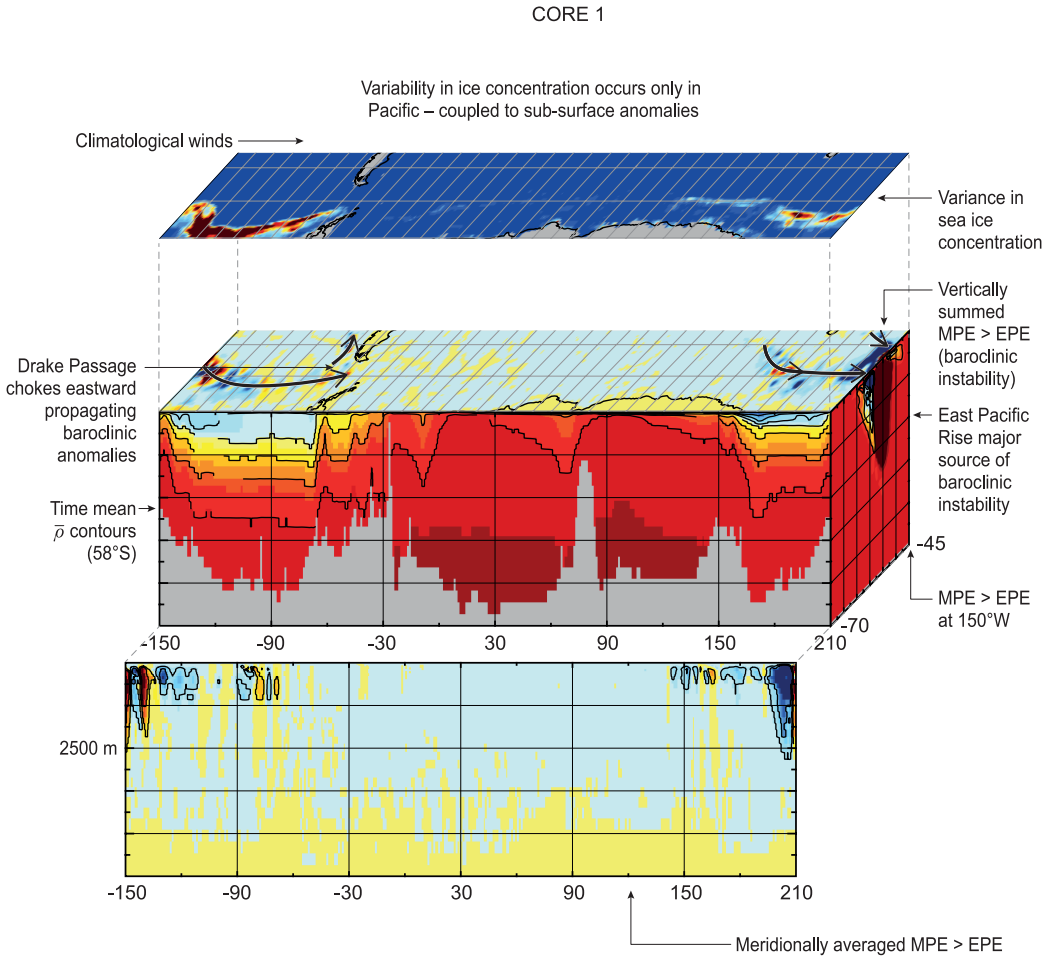

Figure 1: Ocean intrinsic variability (CORE1 forcing). Arrows indicate direction of propagation of disturbances and $\overline{\rho}$ is the time mean density.

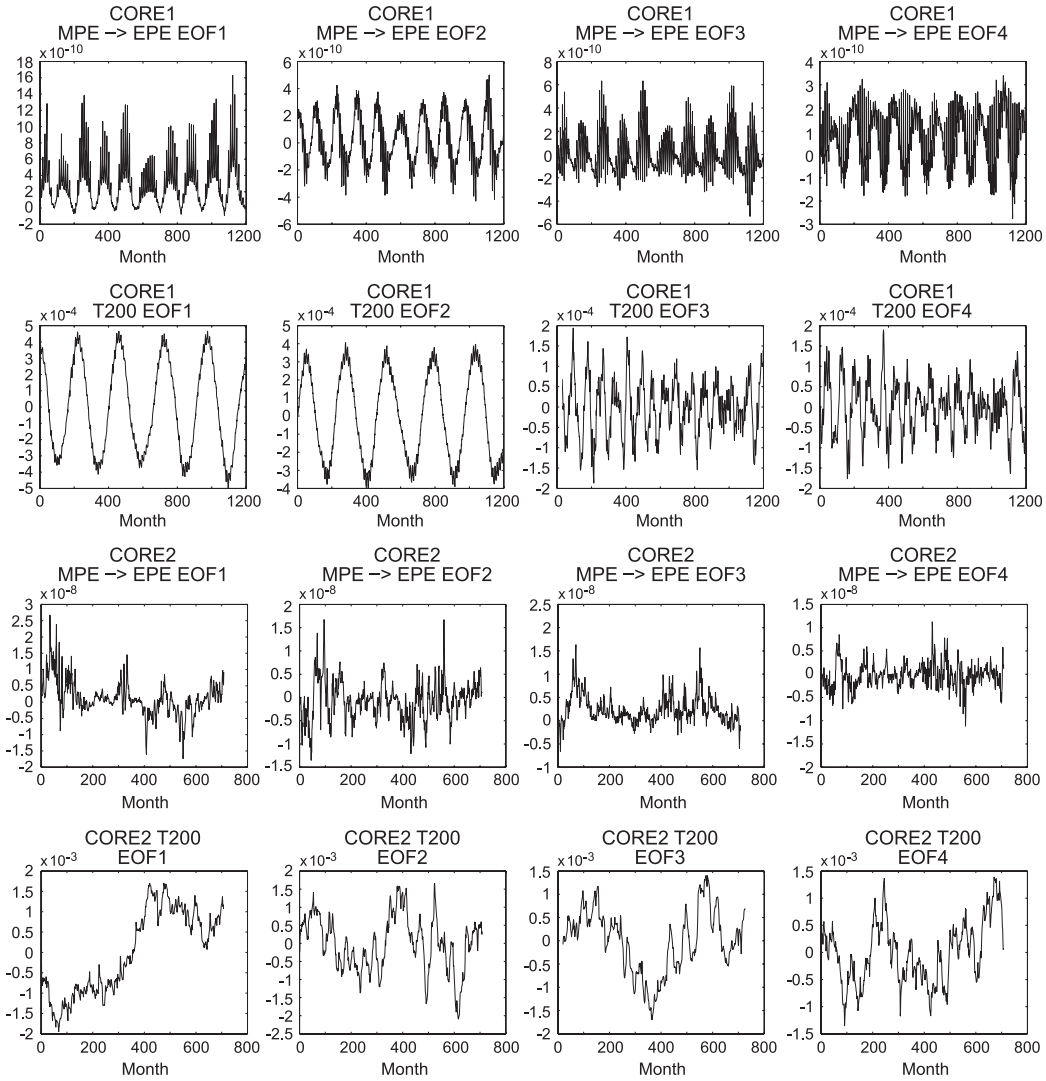

Figure 2: Principal components corresponding to the first four EOFs (left to right). Row one, CORE1 MPE→EPE; row two, CORE1 T200; row three, CORE2 MPE→EPE; row four, CORE2 T200. The 100 year (1200 month) CORE1 simulation is unrelated to any particular date. The CORE2 simulation runs over the 60 year (720 month) period beginning January 1948.

the thermocline is shown by the corresponding PCs of MPE → EPE at a depth of 200 m, which spike during transitions to and from the high and low temperature regimes about every 10 years (Figure 2, row one). A similar PC analysis of the leading modes of variability for barotropic transfers (not shown) reveals maxima corresponding to residence in either the mature warm or cold temperature regimes. Thus, for the Southern Ocean intrinsic mode baroclinic instability is the initiator of regime transitions and barotropic instability is associated with the lifetime of each of the quasi-stationary states.

The corresponding PCs of interannual variability (CORE2) also show marked decadal variability (Figure 2, rows three and four). The CORE2 leading PC for T200 (Figure 2, row four) displays variability characteristic of zonal forcing due to the SAM. PCs two and three characterise the response of the thermocline to latitudinal wind variations due to the ENSO, and PC four describes the variability due to the leading higher order term representative of mid-latitude synoptic weather. The PCs associated with potential energy transfers (Figure 2, row three) show evidence of peaks during transitions between low frequency maxima and minima in T200. However, a simple relationship between baroclinic instability and low frequency variability is not readily apparent.

For the CORE2 (Figure 3) the EOFs of the first two leading modes of variability strongly project onto the Pacific region centred at 150°W, 58°S. EOFs three and five are significant in that they display large variability in a localised region of the Atlantic centred at 0°W, 58°S. The first five EOFs of potential temperature at a pressure of 207 dbars (corresponding to depth 200 m) of the interannual (CORE2, Figure 3) and intrinsic (CORE1, not shown) forcing experiments are similar in the Pacific region, but differ markedly in that for the intrinsic ocean mode there is almost a complete lack of variability outside the Pacific region.

In order to examine how the intrinsic mode responded to the constituent components of the atmospheric forcing over the last 60 years we consider the vertical structure of baroclinic disturbances about the ACC thermocline as

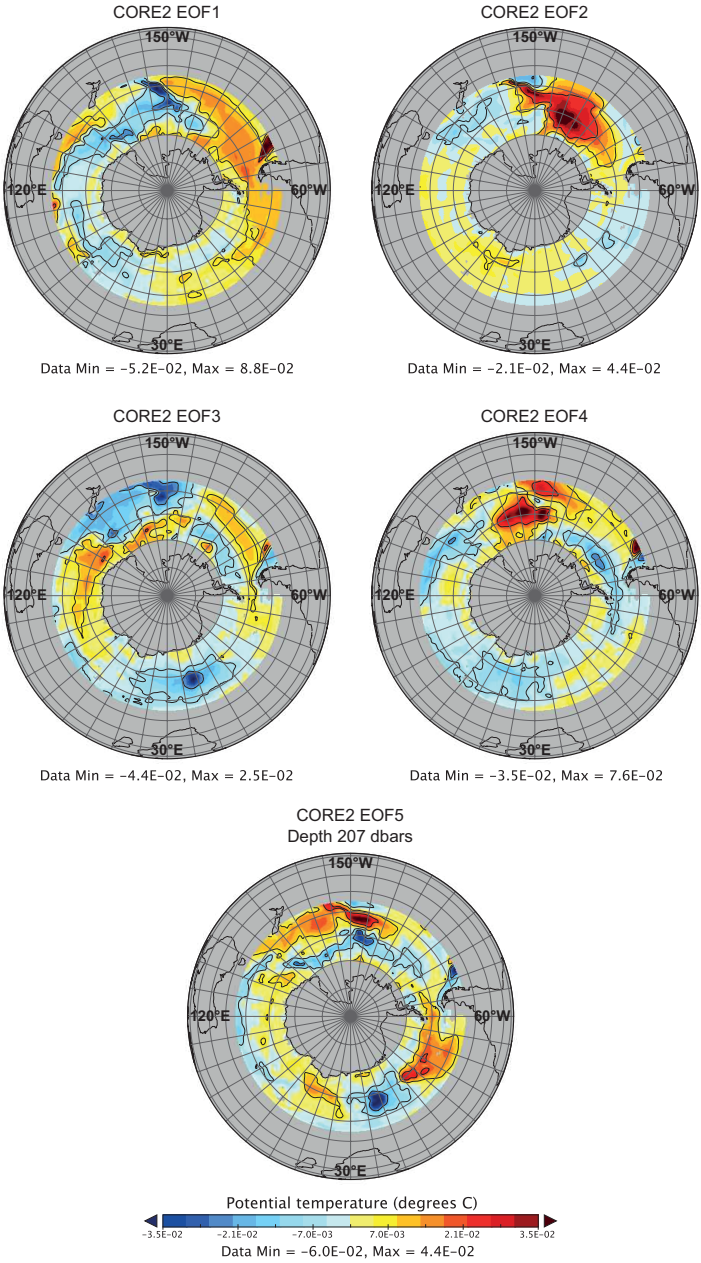

Figure 3: First five EOFs (T200) ocean response to interannual CORE2 forcing. Stereographic projections of continental outlines are overlaid.

sections along 58°S (Figure 4) in experiments in which the ocean is forced with the constituent components of the atmosphere. Figure 4 shows the vertical structure of MPE → EPE for each of the respective forcing experiments. Both the intrinsic ocean (CORE1) and ENSO forced (CORE1+ENSO) experiments show regions of baroclinic disturbances localised about the thermocline in the Pacific (150–130°W) over and downstream of the East Pacific Rise, and in a region along the Chilean coast (60°W). The enhanced vertical extent of baroclinic processes in the ENSO forced case relative to the intrinsic ocean variability clearly demonstrates the role of ENSO in amplifying nascent intrinsic baroclinic instabilities in the Pacific. The increased zonal variability due to SAM forcing (CORE1+SAM) is even more effective at amplifying long timescale disturbancs in the ACC (Figure 4, middle row left column) exhibiting an enhanced signal between 150°E and 180°W, relative to the CORE1 and CORE1+ENSO simulations. The role of the high frequency winds in driving long lived thermocline disturbances is further illustrated in Figure 4 (middle row right column). Here we see an almost equivalent response in the Pacific as the CORE1+SAM case, but now with a significant additional response in the Atlantic near 0°E. We also see evidence of a pathway for baroclinic disturbances between the East Pacific Rise and Drake Passage (60°W) propagating at a depth where the pressure is approximately 800 dbars. Baroclinic processes in the CORE2 may superficially be regarded as a superposition of CORE1 and SAM, ENSO and weather experiments but with the significant addition of an anomaly pathway emanating from the Pacific and teleconnecting to the Atlantic (see also Figure 5). There is no evidence of long timescale baroclinic (or barotropic) processes in the ACC in the greater Indian Ocean between 15–150°E.

5 Summary and conclusions

Our study finds that there exists a nonlinear relationship between model atmospheric forcing, Rossby waves and thermocline disturbances. We demon-

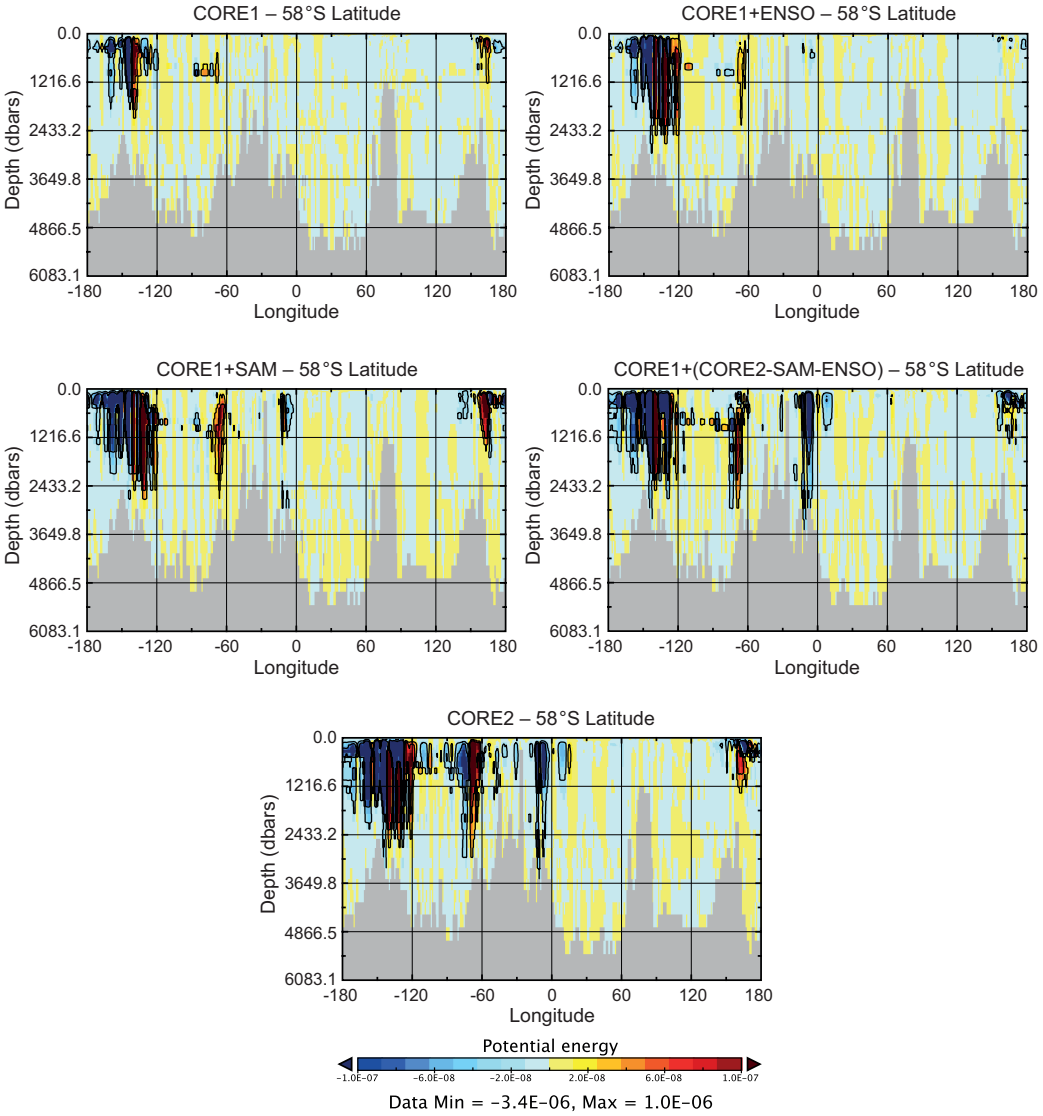

Figure 4: Potential energy transfer along latitude 58°S (equation 1 scaled by $1/g$). Forcing configurations are: top row, CORE1 (left) and CORE1+ENSO (right); middle row, CORE1+SAM (left) and CORE1+CORE2−SAM−ENSO (right); bottom row, CORE2. Units are $10^3\,\mathrm{kg\,m^{-2}s^{-1}}$.

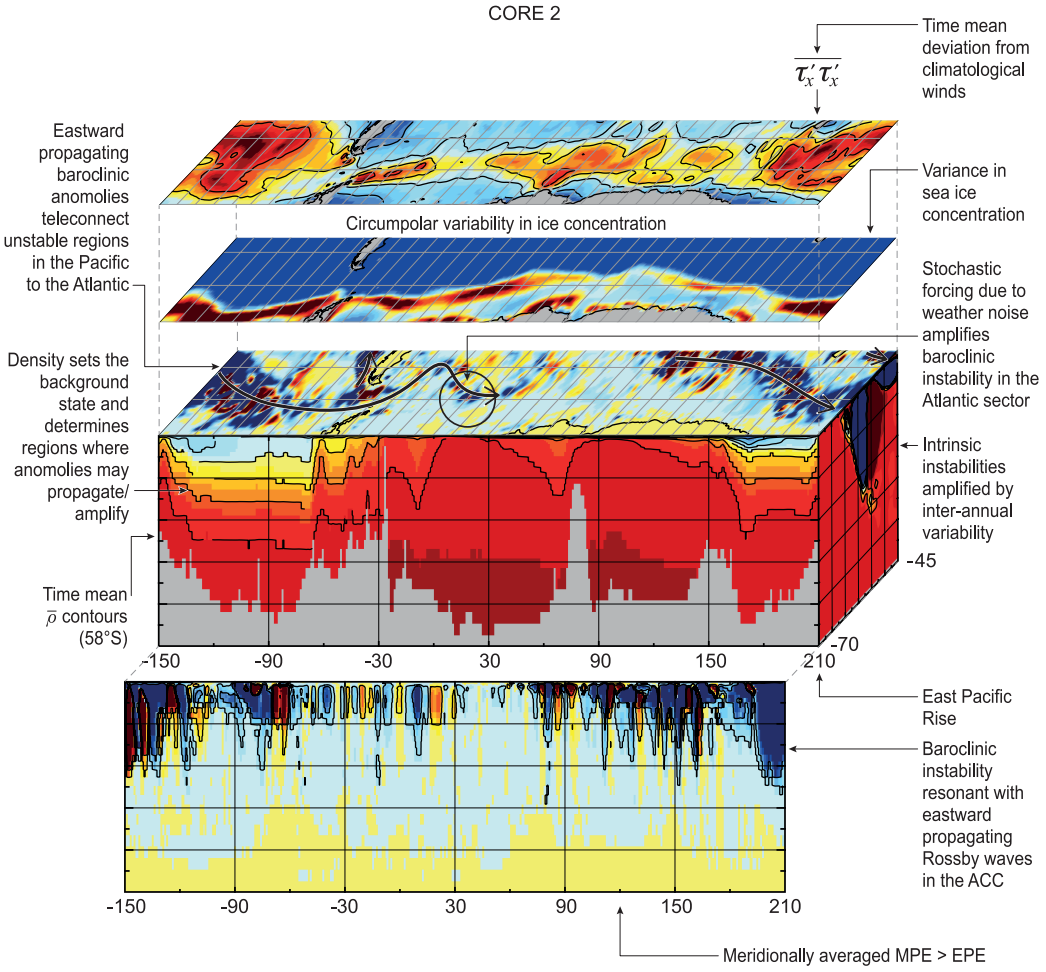

Figure 5: Ocean response to CORE2 interannual forcing. Arrows indicate direction of propagation of disturbances.

strated that decadal scale intrinsic modes of low frequency variability are present in a non-eddy resolving model with sufficient Southern Ocean resolution to resolve Rossby waves and to enable the development of intrinsic low frequency variability in the Pacific sector. We find that large scale coherent wave trains of potential energy transfer structures coincident with significant density gradients are generated in the region of the East Pacific Rise. In contrast, kinetic energy (not shown) was found to be of smaller scale and highly localised with little or no amplitude away from significant topographic peaks at the Rise. Thus we surmise that the intrinsic variability observed in the Pacific arises largely from baroclinic processes. Further, it was shown that the intrinsic mode may be amplified by either or both of the low frequency interannual modes of variability present in the reanalysed atmospheric forcing dataset. In the Pacific, interannual atmospheric modes excite the intrinsic ocean mode with the zonal SAM mode producing the largest amplitude ocean response. In the Atlantic, latitudinal variations due to the ENSO are ineffective at generating significant variability, exciting little or no baroclinic ocean response. In contrast, year to year changes in the high frequency weather patterns are found to be the dominant mechanism driving subsurface disturbances in the Atlantic. High frequency winds also act to excite a significant response in the Pacific.

A Model description

Our ACCESS-o global model configuration is mass conserving and non-Boussinesq. We used pressure coordinates scaled with height in the vertical. Weak restoring was applied to the surface salinity of the top layer (equivalent thickness of 10 m) which was relaxed to World Ocean Atlas (WOA09) fields with a time scale of 60 days to reduce drift. We used the transformed Eulerian mean [6] generalization of the Eliassen and Palm flux approach to model the transport of passive tracers, temperature and salinity, and the K-profile parameterization [4] mixing scheme in the vertical.

We employed the tripolar ACCESS-o model grid: a 360×300 logically rectangular horizontal mesh, overlying an orthogonal curvilinear grid whereby a singularity at the north pole is avoided by using a tripolar grid [7]. This approach also provides reasonably fine resolution in the Arctic Ocean, as well as enhancing computational efficiency. Along the curvilinear 'zonal' direction ACCESS-o has a regular spaced grid with 1° resolution. In the meridional direction the grid spacing is nominally 1° resolution, with the three following refinements:

- tripolar Arctic north of 65°N;
- equatorial refinement to $1/3^\circ$ between 10°S and 10°N;
- a Mercator (cosine dependent) implementation for the Southern Hemisphere, ranging from 0.25° at 78°S to 1° at 30°S.

In the vertical direction there are 50 model levels covering 0–6000 m with a resolution ranging from 10 m in the upper layers (0–200 m) to about 333 m for the abyssal ocean. Although not eddy resolving, this model has sufficient resolution to resolve Southern Ocean Rossby waves and energy transfers associated with transient disturbances that may become resonant with the resolved Rossby waves. Because of the prohibitive computational cost of eddy resolving models and the need for greater than 1000 year spinup runs to achieve steady state, the model resolution described represents a practical compromise to enable the study of decadal to climate timescale ocean dynamics. The spinup used CORE1 forcing with climatological atmospheric fields that were converted to air-sea fluxes with bulk formulas. The initial conditions for temperature and salinity fields came from WOA09, and the model was run until a quasi-steady state with negligible drift was achieved (of the order of 1000 years). The spun up ocean state was used as an initial condition for all experiments reported herein.

References

[1] T. Delworth, A. J. Broccoli, A. Rosati, R. J. Stouffer, V. Balaji, J. A. Beesley, W. F. Cooke, and K. W. Dixon. GFDL's CM2 global coupled climate models. Part 1: Formulation and simulation characteristics. *J. Climate*, **19**:643–674, 2006. doi:10.1175/JCLI3629.1 C203

[2] H. Dijkstra and M. Ghil. Low-frequency variability of the largescale ocean circulation: A dynamical systems approach. *Rev. Geophys.*, **43** RG3002, 2005. doi:10.1029/2002RG000122 C202

[3] C. W. Hughes. Rossby waves in the Southern Ocean: A comparison of TOPEX/POSEIDON altimetry with model predictions. *J. Geophys. Res.*, **100**:15933–15950, 1995. doi:10.1029/95JC01380 C202

[4] W. G. Large, J. C. McWilliams, and S. C. Doney. Oceanic vertical mixing: A review and a model with a nonlocal boundary layer parameterization. *Rev. Geophys.*, **32**:363–403, 1994. doi:10.1029/94RG01872 C213

[5] W. G. Large and S. G. Yeager. Diurnal to decadal global forcing for ocean and sea-ice models: the datasets and flux climatologies. *NCAR Technical Note:*, NCAR/TN-460+STR, CGD Division of the National Centre for Atmospheric Research, 2004. doi:10.5065/D6KK98Q6 C203

[6] T. J. McDougall and P. C. McIntosh. The temporal-residual-mean velocity. Part I: Derivation and the scalar conservation equations. *J. Phys. Oceanogr.*, **26**:2653–2665, 1996. doi:10.1175/1520-0485(1996)026<2653:TTRMVP>2.0.CO;2 C213

[7] R. J. Murray. Explicit generation of orthogonal grids for ocean models. *Journal of Computational Physics*, **126**:251–273, 1996. doi:10.1006/jcph.1996.0136 C214

[8] A. B. Pezza, H. A. Rashid, and I. Simmonds. Climate links and recent extremes in antarctic sea ice, high-latitude cyclones, southern annular

mode and ENSO. *Climate Dynamics*, **38**:57–73, 2012. doi:10.1007/s00382-011-1044-y C203

[9] G. Quattrocchi, S. Pierini, and H. A. Dijkstra. Intrinsic low-frequency variability of the gulf stream. *Nonlinear Processes in Geophysics*, **19**:155–164, 2012. doi:10.5194/npg-19-155-2012 C202

[10] A. Timmermann. Changes of ENSO stability due to greenhouse warming. *Geophys. Res. Let.*, **28**:2061–2064, 2001. doi:10.1029/2001GL012879 C203

Author addresses

1. **Terence J. O'Kane**, CSIRO Marine and Atmospheric Research, Hobart, Tasmania 7001, Australia.
   mailto:terence.okane@csiro.au
2. **Richard J. Matear**, CSIRO Marine and Atmospheric Research, Hobart, Tasmania 7001, Australia.
3. **Matthew A. Chamberlain**, CSIRO Marine and Atmospheric Research, Hobart, Tasmania 7001, Australia.
4. **James S. Risbey**, CSIRO Marine and Atmospheric Research, Hobart, Tasmania 7001, Australia.
5. **Ilia Horenko**, Universita della Svizzera Italiana, Lugano, Switzerland.
6. **Bernadette M. Sloyan**, CSIRO Marine and Atmospheric Research, Hobart, Tasmania 7001, Australia.